Novel UHF RFID tag structure based on polycarbonate material, for renewable energy applications

Zakaria Errachidi, Jamal Zbitou, Mohammed El Gibari, Noha Chahboun

Novel UHF RFID tag structure based on polycarbonate material, for renewable energy applications

Zakaria Errachidi [1*], *Jamal* Zbitou[2], *Mohammed* El gibari[3], and *Noha* Chahboun[1]

[1] LABTIC, ENSA of Tangier, Abdelmalek Essaadi University, Tetouan, Morocco
[2] ENSA of Tetouan, Abdelmalek Essaadi University, Tetouan, Morocco
[3] IETR, UMR CNRS 6164, Nantes, France

Abstract. In the renewable energy sector, the management of protective equipment (PPE and collective safety systems) is a crucial priority to reduce workplace risks and ensure the safety of operations. This article presents the design and optimization of a novel UHF RFID tag operating at 868 MHz, featuring an original structure inspired by a wind turbine shape. This tag is specifically designed to be integrated into industrial safety helmets made of polycarbonate, a material characterized by a dielectric constant εr = 2.9 and a loss tangent tanδ = 0.01. The tag aims to enhance equipment tracking and traceability. The antenna is adapted to an Alien H4 UHF RFID chip, which has an internal impedance of Z = 23.37 - j203.3 Ω at the chosen frequency, ensuring optimal power transfer. Simulation results demonstrate that the tag offers high readability and efficiency while respecting the mechanical and dielectric properties of polycarbonate. This study highlights the potential of innovative UHF RFID tag designs for tracking safety equipment in industrial environments, offering a robust solution to improve workplace safety and operational efficiency.

1 Introduction

Ultra-High Frequency (UHF) RFID technology has established itself as a fundamental element for asset tracking and management [1], particularly in industrial environments where protection against electrical and mechanical risks is a top priority. One of its notable applications is the integration of RFID tags into safety equipment, such as helmets, which represents a unique opportunity to enhance worker safety and optimize operations. However, designing these tags involves addressing several challenges, including the material properties of the equipment and the harsh conditions found at industrial sites [2].

In this study, we propose a new UHF RFID tag operating at 868 MHz, featuring a windmill-inspired structure optimized for integration into polycarbonate safety helmets, as shown in Figure 1. Polycarbonate is one of the most commonly used materials in helmet manufacturing, valued for its unique combination of lightness, impact resistance, and insulating properties. These characteristics make it an ideal choice for environments exposed to high electrical risks; however, they also impose specific constraints on tag design, particularly regarding mechanical compatibility and dielectric performance.

The windmill-inspired design not only enhances the tag's aesthetics but also improves its functionality by optimizing radiation efficiency and read range. This study demonstrates the feasibility of integrating RFID technology into safety helmets, providing a practical solution for real-time tracking and management of safety equipment in industrial environments [3]. By combining innovative design with material-specific optimization, this work paves the way for broader applications of RFID technology in workplace safety and beyond

Fig. 1. A safety helmet equipped with the proposed RFID tag.

2 UHF RFID Design

The proposed structure is inspired by the shape of a wind turbine and consists of two dipoles, each loaded with a triangular split-ring resonator (T-SRR), representing the turbine blades. At the centre of this structure, an inverted T-shape, featuring a T-match network symbolizing the

* Corresponding author: errachidi.zakaria@gmail.com

turbine mast, has been added to facilitate impedance matching between the antenna and the RFID chip, which is integrated in the middle of the tag. This unique configuration optimizes power transfer while enhancing radiation performance. Figure 2 illustrates the geometry of the proposed tag, and Table 1 provides its dimensions.

The triangular split-ring resonators (T-SRR) contribute to broadening the bandwidth and improving the antenna's efficiency, while the T-match structure ensures precise impedance matching with the Alien H4 RFID chip [4], thereby guaranteeing reliable communication and an extended read range. This innovative design, combining aesthetics and functionality, provides a high-performance solution tailored for demanding industrial environments.

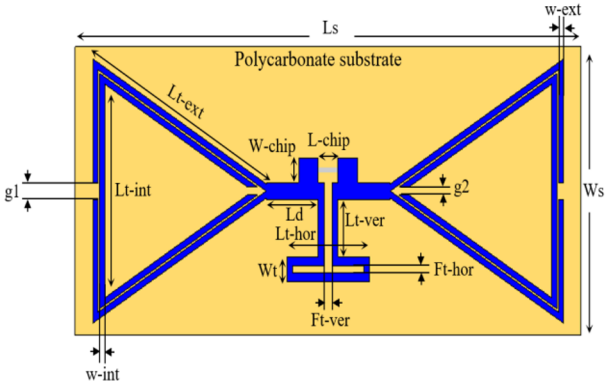

Fig. 2. Geometry of the proposed UHF RFID antenna with optimized parameters

Table 1. dimensions of the optimized parameters.

Parameter	Dimension (mm)	Parameter	Dimension (mm)
Lt-ext	30.3	Lt-hor	12.5
Lt-int	25.1	Lt-ver	7
w-ext	0.75	Ft-hor	0.9
w-int	0.65	Ft-ver	1.2
g1	2	Ld	7.9
g2	1	W-chip	3
Wt	3	L-chip	3
Ls	80	Ws	40

The proposed structure is specifically designed to accommodate an Alien Higgs 4 UHF RFID chip integrated into a standard strap packaging, whose characteristic impedance is Z_{chip}=23.27−j203.35 Ω at the frequency of 868 MHz. To model the behavior of this chip during simulations performed with CST Microwave Studio software, the microchip was replaced by a series RC dipole. This dipole consists of a resistance Rs=23.27 Ω, representing the real part of the impedance, and a capacitance Cs=0.9016 pF, which corresponds to the capacitive imaginary part (−j203.35 Ω) at the operating frequency [5-6]. This modeling faithfully reproduces the electrical properties of the Alien H4 chip, taking into account its frequency response and complex impedance characteristics.

3 Theoretical Study of a Triangular SRR Cell

SRRs, used in metamaterials, enable the manipulation of unusual electromagnetic properties, such as negative permittivity and permeability. These characteristics pave the way for advanced applications in telecommunications, including miniaturized antennas (e.g., RFID tags) [7], filters, and stealth systems.

In this study, we used triangular-shaped SRRs in our structure. Figure 3 illustrates the geometry of a unit cell of the Triangular-SRR. It is important to note that several geometric shapes are commonly studied in this field, particularly square and circular shapes, which are the most widely used due to their effectiveness in numerous applications [8-10].

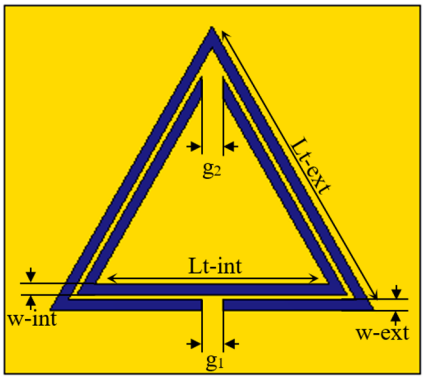

Fig. 3. Unit cell of Triangular-SRR.

3.1 Resonant frequency of the Triangular-SRR:

The resonant frequency of the triangular SRR can be calculated using the equations (1), (2), (3), and (4) [11-13].

$$f_{0tsrr} = \frac{1}{2\pi\sqrt{L_{eq}C_{eq}}} \quad (1)$$

$$C_{eq} = 0.75.lt.C_{pul} \quad (2)$$

$$C_{pul} = \frac{\sqrt{\varepsilon_{eff}}}{C_0 Z_0} \quad (3)$$

$$L_{eq} = \frac{3\,\mu_r\,\mu_0}{2\pi}\left(ln\left(\frac{lt}{w}\right) - 1.405\right) \quad (4)$$

Where:

- L_{eq} and C_{eq} are inductance and capacitance of the unit cell.
- Zo is the impedance of the medium.
- C_{pul} is the capacitance per unit length, between the rings.
- l_t and w are wire length and width respectively.
- $c_0 = 3\times10^8$ m.s^{-1} is the speed of light in free space

4 Parametric Study of the Proposed RFID TAG

4.1 Effect of Substrate Length (Ls) Variations

The frequency evolution of the reflection coefficient of the RFID tag as a function of the variation in its substrate length (Ls) is shown in Figure 4. All parameters remain fixed, except for (Ls), which varies from 73 mm to 89 mm, we can observe that when (Ls) decreases from 80 mm to lower values, the resonant frequency shifts toward higher frequencies with a reduction in its magnitude. On the other hand, when (Ls) increases from 80 mm to higher values, the S11 parameter remains almost stable at the frequency of 868 MHz, with an improvement in its magnitude.

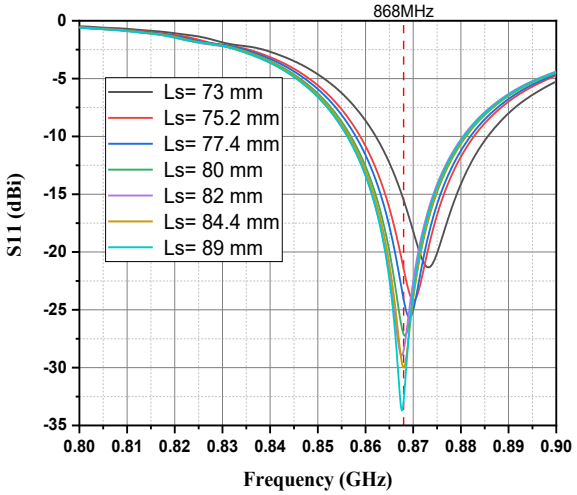

Fig. 4. Simulated reflection coefficient for different values of LS.

4.2 Effect of Substrate Width (Ws) Variations

Regarding the effect of the substrate width variation on the resonant frequency and the reflection coefficient, we fixed the length at 80 mm and varied the width from 36 mm to 52 mm. According to Figure 5, we observed a very slight shift in the curve around the operating frequency of 868 MHz.

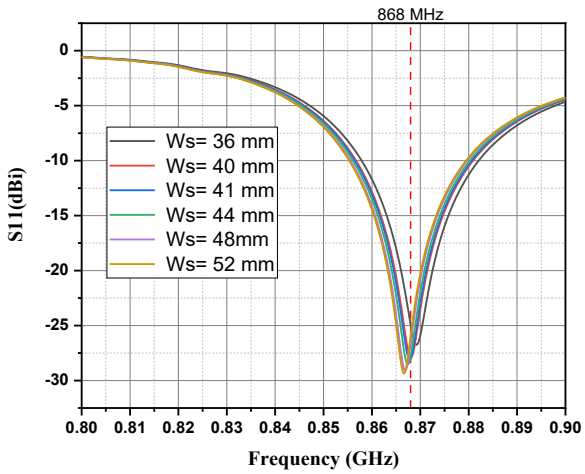

Fig. 5. Simulated reflection coefficient for different values of Ws.

4.3 Effect of the Outer Triangle Side Length (Lt-ext)

This study aims to analyse the effect of the dimensions of the triangular split-ring resonator (SRR) on the variation of the reflection coefficient and the resonance frequency. A variation in the length of the outer triangle side of the resonator was performed. As shown in Figure 6, the S11 parameter significantly affected when the length Lt-ext is increased or decreased. At a value of 30.3 mm, we achieved the desired matching point.

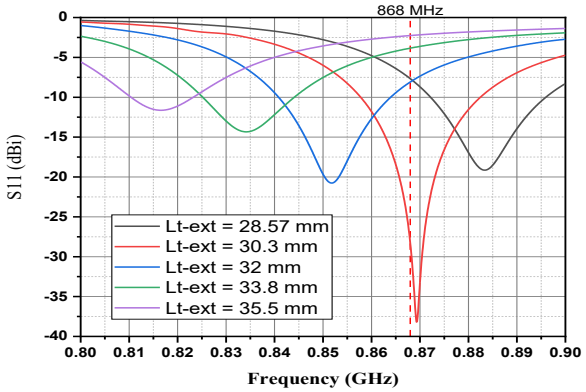

Fig. 6. Simulated reflection coefficient for different values of Lt-ext.

5 Simulated results and discussions

This section presents the simulated results of the tag antenna, highlighting the optimized parameters. The simulations were conducted using CST Microwave Studio software, enabling the analysis of the antenna's electromagnetic performance and validating its behavior prior to the fabrication and practical testing.

The simulation of the reflection coefficient (S11) is illustrated in Figure 7. The simulated curve shows significant attenuation at the operating frequency of 868 MHz, reaching -32,88 dBi, indicating excellent impedance matching between the RFID tag and the chip. This matching is crucial for ensuring optimal energy transfer and maximizing system performance. This excellent matching is also clearly visible in Figure 8, which shows an antenna impedance of Zant = 25 + j202,06 Ω, very close to the conjugate of the chip's impedance, thereby confirming the effectiveness of the proposed design.

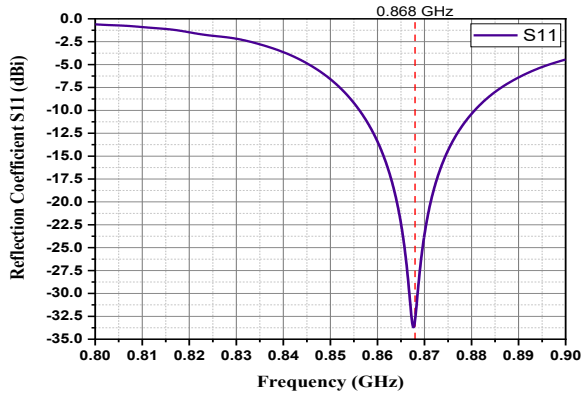

Fig. 7. The simulated reflection coefficient S11 with optimized parameters

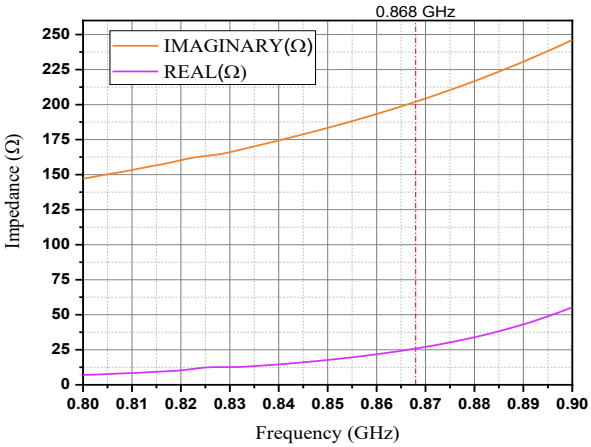

Fig. 8. The simulated input impedance of the RFID antenna with optimized parameters.

Moreover, the tag provides a bandwidth of approximately 24.5 MHz at -10 dB, covering a range from 855.9 MHz to 880.4 MHz, as shown in Figure 9. This allows it to fully meet the requirements of the European frequency band dedicated to RFID, which ranges from 865 MHz to 868 MHz.

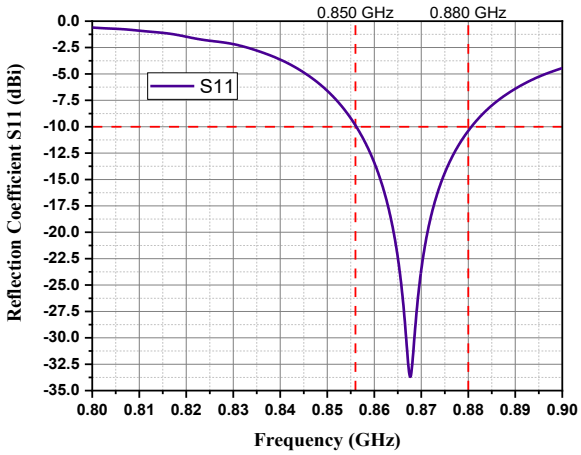

Fig. 9. The simulated bandwidth at -10 dBi.

The read distance of an RFID tag is a key indicator of its efficiency, representing the maximum range at which the tag can communicate with an RFID reader. The Friis formula, modelled by Equation (5), was used to calculate this distance [14].

$$Rr = \frac{c}{4\pi f}\sqrt{\frac{EIRP.G_t.\tau}{P_{th}}} \quad (5)$$

Where:
EIRP (Effective Isotropic Radiated Power) is fixed at 3.3 W in the European band ([865-868] MHz).
c represents the speed of light 3×10^8 m/s.
f is the central operating frequency (868 MHz).
P_{th} is micro-chip's sensitivity, it is -20.5 dBm for the Alien H4 strap micro-chip.

The read range is also influenced by other factors related to the tag's design, particularly the impedance matching between the tag's antenna and the chip. This adaptation can be verified and calculated using Formula (6) for τ. The closer the value of τ is to 1, the better the adaptation is ensured [14]. For the studied antenna, the calculated value of τ reaches 0.99.

$$\tau = 1 - |S_{11}|^2 = 1 - \left|\frac{Z_c - Z_a^*}{Z_c - Z_a}\right| = \frac{4R_cR_a}{|Z_c - z_a|^2} \leq 1 \quad (6)$$

Figure 10 illustrates the variation of the tag's gain as a function of frequency. This parameter, among others, plays a crucial role in determining the quality of the design and, more specifically, in the reading range. At the resonance frequency, the gain reaches its maximum value of 1.72 dBi. This value aligns with that shown in Figure 11, which presents the tag's radiation pattern. The radiation pattern is omnidirectional in the yz-plane (phi = 90°) and bidirectional in the xz-plane (phi = 0°) at the frequency of 868 MHz.

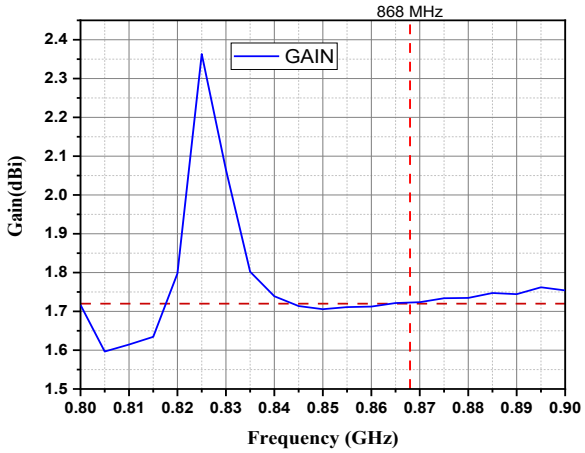

Fig. 10. Simulated gain of the proposed RFID tag antenna.

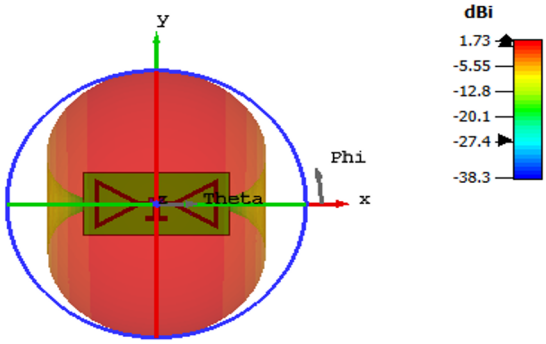

Fig. 11. Radiation pattern-3D of the UHF RFID Tag at 868 MHz.

After applying the Friis formula, the read range is illustrated by the curve shown in Figure 12. It can be observed that at the resonance frequency, this distance reaches a maximum value of around 21 meters.

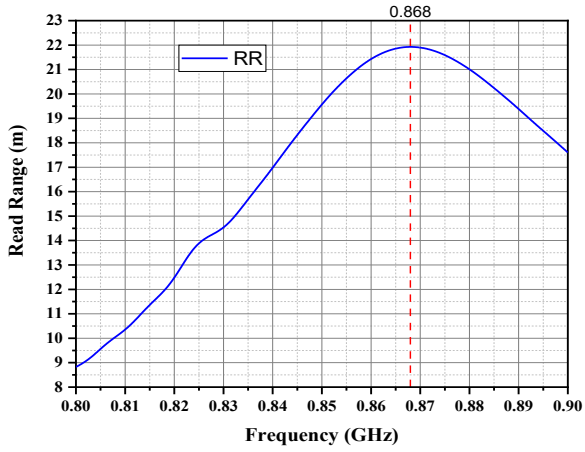

Fig. 12. Simulated Read Range of the proposed RFID tag antenna.

6 Conclusion

In this study, we chose a triangular shape to design our SRRs (Split Ring Resonators), which are coupled to a dipole loaded with a T-match network to ensure flexible matching. This shape is inspired by a wind turbine. The objective of this study is to design an RFID tag that can adapt to a substrate made of polycarbonate, a material commonly used in the manufacturing of safety helmets. Our findings show remarkable effectiveness, particularly in terms of impedance matching between the tag and the Alien H4 chip, as well as a read range reaching 21 meters. Furthermore, we aim to broaden research perspectives by comparing its performance with that of more traditional shapes

References

1. L. Dhingra, M. S. Reddy, L. A. Deshpande, V. J. Vijayalakshmi, R. Saini, X. M. Raajini ,Utilizing Real-Time Tracking with RFID Technology. 15th International Conference on Computing Communication and Networking Technologies (ICCCNT), (2024).
2. T. Aleong, K. F. Pun, Advancing the Ultra High Frequency RFID in Industrial Applications: A Review. The West Indian Journal of Engineering, Vol.44, No.1, (2021)
3. L. Cui, Z. Zhang, N. Gao, Z. Meng, and Z. Li, Radio frequency identification and sensing techniques and their applications. A review of the state-of-the-art," Sensors 2019, 19, 4012, (2019)
4. M. T. Reich, C, Bauer-Reich, UHF RFID Impedance Matching: When is a T-Match Not A T-Match? IEEE International Conference on RFID (IEEE RFID), 2014.
5. (2016). Higgs 4 RFID IC | Alien Technology. Accessed: Oct. 8,2018. [Online]. Available: https://www.alientechnology.com/products/ic/higgs-4/
6. Z. Errachidi, J. Zbitou, M. Latrach, A. Lakhssassi, A. Oukaira, N.Chahboun,A New Design of a Spiral UHF RFID Tag Dipole Antenna Mounted on Metallic Objects. IEEE 22nd Mediterranean Microwave Symposium (MMS). October 30 to November 01, (2023)
7. Z. Errachidi, J. Zbitou, N.Chahboun, A. Oukaira, Y. Laaziz, Miniaturized UHF RFID Tag Based on Dipole Antenna Loaded with Hexagonal Split Ring Resonators (H-SRR), Mounted on Metallic Objects. The first International Conference on Computing, Internet of things and Microwave Systems (ICCIMS 2024) July 29-31, (2024)
8. Prahlad, B. K. Sujataha, M. R. Ahmed, Concepts of Antenna Design for RFID Systems: A review and a practical Application. TechRxiv. August 09, (2022).
9. R. Marques, F. Mesa, J. Martel, and F. Medina, Comparative Analysis of Edge- and Broadside-Coupled Split Ring Resonators for Metamaterial Design—Theory and Experiments. IEEE trans on Antennas and Propagation, vol. 51, no. 10, (2003).
10. C. Saha, J. Y. Siddiqui, A Comparative Analyis for Split Ring Resonators of Different Geometrical Shapes. 2011 IEEE Applied Electromagnetics Conference (AEMC). (2012).
11. K. Mahendran, R. Gayathri, H. Sudarsan, Design of multi band triangular microstrip patch antenna with triangular split ring resonator for S band, C band and X band applications. Microprocessors and Microsystems, Vol 80, (2021) https://doi.org/10.1016/j.micpro.2020.103400
12. A. K. Vallappil, B. A. Khawaja, M. K. A. Rahim, M. N. Iqbal, H. T. Chattha, "Metamaterial-Inspired Electrically Compact Triangular Antennas Loaded with CSRR and 3x3 Cross-Slots for 5G Indoor Distributed Antenna Systems," Micromachines, 13, 198, (2022). https://doi.org/10.3390/mi13020198
13. P. Rajalakshmi, N. Gunavathi, Compact Complementary Folded Triangle Split Ring Resonator Triband Mobile Handset Planar Antenna for Voice and Wi-Fi Applications. Progress In Electromagnetics Research C, Vol. 91, 253–264, (2019)
14. F. K. Byondi, C. H. Sul, Y. Chung , Super Long Range Small Empty Cavity UHF RFID Tag Antenna Design for a Metal Cart. IEEE Region Ten Symposium (Tensymp), (2018).